

Short Communication

Effect of Curing Temperature on Corrosion Resistance of a Chromium-free Coating on Hot Dip Galvanized Steel Sheet

Shan Liu¹, Zhefeng Xu^{2,3}, Jianhong Yi^{3,*}

¹ Department of Biological and Chemical Engineering, Panzhihua University, 617000, Panzhihua, P.R. China.

² PanGang Group Research Institute Co., Ltd., State Key Laboratory of Vanadium and Titanium Resources Comprehensive Utilization, Panzhihua 617000, Sichuan, P.R. China.

³ Faculty of Materials Science and Engineering, Kunming University of Science and Technology, Kunming 650093, P.R. China.

*E-mail: chuannong2010@126.com

Received: 26 February 2018 / Accepted: 16 April 2018 / Published: 5 June 2018

In this work, tannic acid powder, fluoro titanate solution and colloidal silica were used to prepare a coating on a hot dip galvanized steel sheet. The pH value of the passivating solution ranges between 2~7, and the curing temperature is 20 °C, 60 °C, 80 °C and 100 °C. The interface connectivity of the coating was investigated using a Fourier transform infrared spectrometer. Microstructures of the coating were observed using a field-emission scanning electron microscope equipped with an energy dispersive spectrometer and an X-ray photoelectron spectrometer. The corrosion resistance of the coating was studied using an electrochemical workstation. The results show that the coating thickness increased with increasing curing temperature. A coating thickness of 0.62 μm is achieved with a curing temperature of 100 °C; at this temperature, the corrosion potential E_{corr} is 410.5 mV, and the polarization resistance (R_p) is $2.13 \times 10^6 \text{ cm}^{-2} \text{ ohms}$. These conditions provided the best corrosion resistance of the coating.

Keywords: Curing temperature; hot dip galvanized steel sheet; coating; corrosion resistance; microstructure

1. INTRODUCTION

Hot dip galvanizing is an effective way to improve the corrosion resistance of iron and steel surfaces and is widely used on vehicles, building materials, home appliances, shipbuilding, machinery and many other fields[1]. However, hot dip galvanized steel rolls inevitably suffer corrosion and generate white rust from long-term exposure to industrial and marine atmospheres during the storage

and transportation processes from production to customer use[2]. An important solution for preventing the formation of white rust is to produce a passive film with a certain thickness on the surface of hot dip galvanized steel sheet by coating[3,4].

Conventionally, hot dip galvanized steel coating is generated by hexavalent chromate[5]. However, studies showed that hexavalent chromium ion is highly toxic and carcinogenic and is damaging to the environment [6,7]. At present, most domestic enterprises depend on the environmental protection passivation solution product of Parkerizing Co., LTD. and Henkel [2,8], which are lacking in independent study and reproducibility. The costs of these products are substantially high due to their proprietary nature, the higher prices of imported products, and the crude quality and stability of domestic products [9]. To solve the key problems and overcome the technical difficulties, domestic researchers have studied inorganic salts such as trivalent chromium, titanium, zirconium and molybdic acid salt, as well as organic solutions such as phosphoric acid, isopropyl alcohol, TERT butanol and tannic acid[10]. Based on these research studies [6,7,10,11,13], this paper selected tannic acid powder, titanium fluoride solution and colloidal silica sol as raw materials. Fourier transform infrared spectrometer (FTIR), scanning electron microscope, X-ray photoelectron spectrometer and electrochemical workstation were used as methods to study the passivating coating binding interface, microstructure and corrosion resistance under different curing temperatures, providing a reference for environmental protection passivation solutions and passivation mechanisms.

2. EXPERIMENTAL MATERIALS AND METHODS

A 75 mm × 150 mm × 2 mm commercial hot dip galvanized steel sheet (DX54D+Z, Pan Steel Co., China) was selected as the substrate material, with a composition of C < 0.01%, Mn < 0.30%, P < 0.020%, S < 0.015%, Cu < 0.15%, Ni < 0.15%. First, the specimen was dipped into a 10% skim soak for 1 minute to remove the dust and oil on its surface. Second, the specimen was wiped clean with fat-free cotton and dried in an oven at 100 °C for 10 minutes. Third, 500 ml of deionized water, 30~60 g tannic acid powder (98%, Chengdu Kelong), 2~5 mL H₂TiF₆ solution (99%, Sigma-Aldrich) and 50~100 g colloidal silica sol (pH 7.0~8.0, particle size 10~16, 35%, Dow) were added successively and blended into a homogeneous phase solution by quickly stirring at room temperature, and the pH value of this solution was controlled between 2 and 7.

During the experiment, the pretreated specimen of the hot dip galvanized steel sheet was dipped into the solution for 1 s and then dried and cured under temperatures that increased from 60 °C to 100 °C at 60-second intervals[5,7,8]. The coating thickness was measured using a nondestructive Fisher device (Dual Scope MP40 model), and each sample was measured at 3 points, with the average of those points reported as the sample thickness. The relationship between curing temperature and coating thickness is shown in Table 1.

Table 1. Relationship between curing temperature and coating thickness

Trials	Film thickness (μm)	Surface treatment agent
20 °C	0	0
60 °C	0.58	tannic acid - H_2TiF_6 / KH792 sol
80 °C	0.60	tannic acid - H_2TiF_6 / KH792 sol
100 °C	0.62	tannic acid - H_2TiF_6 / KH792 sol

The interface connectivity of the coating was analyzed with Fourier transform infrared spectrometer (AVATAR-360, FT-IR, wavenumber range from 4400~400 cm^{-1} , solid KBr pellet), with a resolution of 2 cm^{-1} and a wavenumber range between 500 and 4000 cm^{-1} . The measurements were performed in Attenuated Total Reflectance (ATR) geometry by means of a diamond Internal Reflection Element (IRE). The microstructure of the coating was observed using a field-emission scanning electron microscope equipped with an accelerating voltage of 15 kV (Shimadzu SS-550, Japan), with an energy dispersive spectrometer Shimadzu EDS facility. Chemical composition analysis of the sample surface layer was performed with an X-ray photoelectron spectrometer (ESCALAB 250Xi) system. Wide scans and detailed scans (pass energy 20 eV) of Zn 2p, ZnM, Cl 2p, S 2p, C 1s, and O 1s were done using a monochromatic Al $K\alpha$ X-ray source (1486.6 eV) operated at 300 W (15kV/20 mA). Measurements were taken over two different areas of analysis, each approximately 0.4 mm^2 in size. The corrosion resistance of the coating was studied using a CHI650A type electrochemical workstation with a three-electrode system, a saturated calomel electrode as the reference electrode, a 213 platinum electrode as the auxiliary electrode, and a 3.5% NaCl solution as an electrolyte. The electrochemical cell consisted of a working electrode with 1 cm^2 exposure area of the sample. The scan rate for potentiodynamic linear polarization (LPR) was 1 mV/s . The salt spray test was performed in a chamber containing 5.0 wt% NaCl fog according to the ASTM B117-03 standard [7]. The percentage of the corroded area was recorded at intervals of 24 h, and the result was based on the average of three samples of the HDG steel coated at different curing temperatures and with different coating thicknesses.

3. RESULTS AND DISCUSSION

3.1 IR spectra of passivating solution and coating

The IR spectra of passivating solution and coating before and after curing are shown in fig. 1. In the figure, curve a is the IR spectrum of the coating, while curve b is the IR spectrum of the passivating solution. In curve a, there is a broadening phenomenon at a wavenumber of 3452 cm^{-1} , which is the -OH stretching vibration peak, indicating that the solution after hydrolysis had an Si-OH group. A wavenumber of 2099 cm^{-1} corresponds to the C-H absorption peak generated by CH_2 in

silane stretching, a wavenumber of 1643 cm^{-1} corresponds to the $-\text{NH}_2$ stretching vibration peak, a wavenumber of 1419 cm^{-1} represents CH_3 and CH_2 stretching peaks, and a wavenumber of 1098 cm^{-1} is the stretching vibration peak of Si-O-Si or Si-O-C groups, indicating that some silanol condensation reaction occurred in the solution. In addition, a wavenumber of 915 cm^{-1} indicates that due to the presence of Si-OH , generated from the Si-O group, the widened peak at a wavenumber of 689 cm^{-1} is the stretching vibration peak of CH_2 and CH_3 in the $-\text{Si-OC}_2\text{H}_5$ group, indicating incomplete silane hydrolysis.

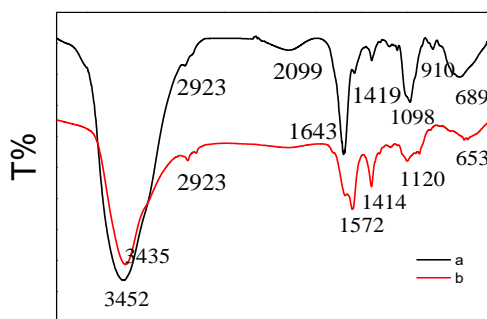


Figure 1. IR spectra of passivating solution and coating

Compared with curve a, a stretching vibration peak occurred at 3435 cm^{-1} in curve b, indicating the incomplete condensation of silanol Si-OH . A wavenumber of 2923 cm^{-1} , which is the absorption peak of C, and the broadening phenomenon at 1572 cm^{-1} , which corresponds to the $-\text{NH}_2$ stretching vibration peak and CO symmetric/asymmetric stretching vibration peak, indicated that NH_4 , epoxy bond and $-\text{COOH}$ exist in the passivating coating. A wavenumber of 1414 cm^{-1} corresponds to CH_2 and CH_3 , and a wavenumber of 1120 cm^{-1} corresponds to the stretching vibration peak of Si-O-Si , which also shows broadening. According to the elements on the surface of hot dip galvanized steel sheet, it can be inferred that this wide phenomenon resulted from the overlap of Si-O-Si and Si-O-Zn absorption peaks[12].

Analyses of the comparison of the IR spectra of passivating solution and coating before and after curing used a certain reference value to reveal the mechanism of the adhesion and reaction of coating. Instead of simple physical deposition, an Si-O-Zn bond was generated through a chemical bonding reaction at the interface of passivating solution and hot dip galvanized steel sheet, and an Si-O-Si bond was formed by condensation from silicon alcohol Si-OH , which means passivating materials and processes can form coatings on the surface of hot dip galvanized steel sheets.

3.2 Effect of curing temperature on the quality of coating

To further examine the effect of curing temperature on coating quality, the surface morphologies of coatings cured at different temperatures were examined with an electron microscope (ShimadzuSS-550, Japan). The micrograph results are shown in fig. 2. Fig. 2 (a) and (b) show micro zone morphologies of a $0.58\text{ }\mu\text{m}$ coating formed under a curing temperature of $60\text{ }^\circ\text{C}$. As shown in

these figures, there are tiny scaly protrusions, and the coating was not homogeneous or dense, indicating an incomplete curing process.

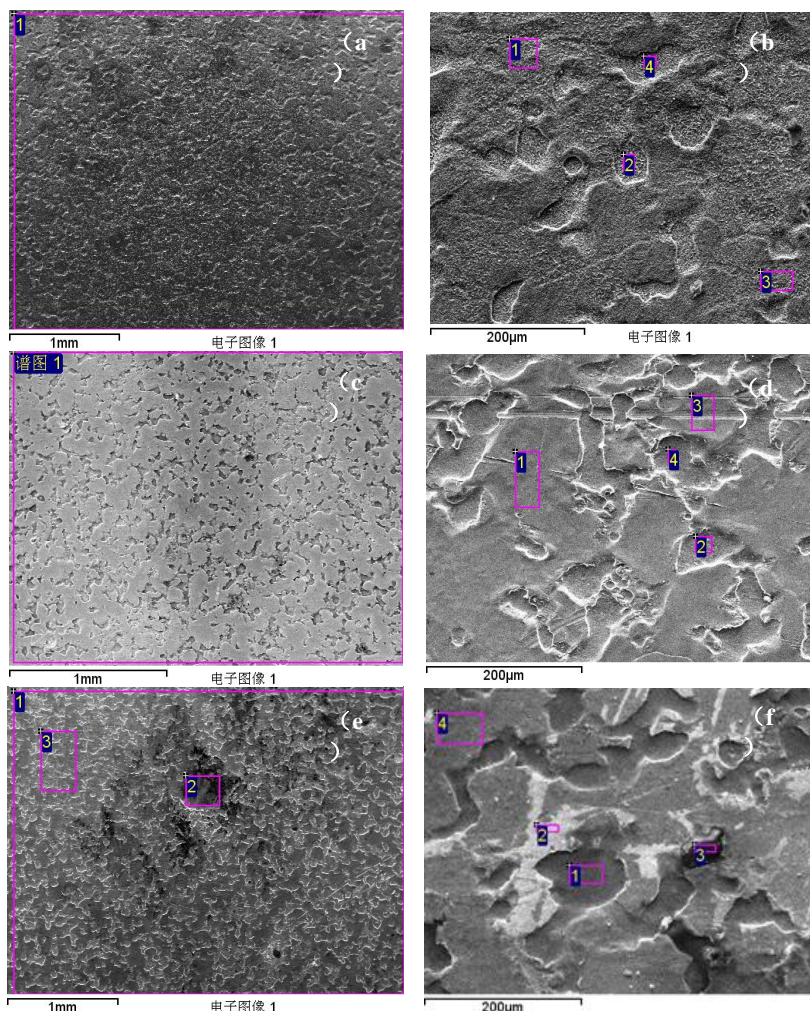


Figure 2. SEM analysis of coating microstructure

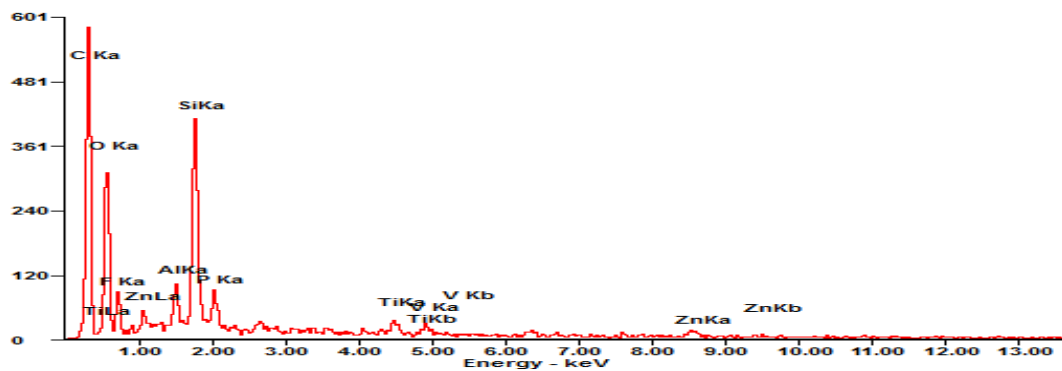


Figure 3. EDS analysis of coating microstructure

Fig. 2 (c) and (d) show that the micro zone morphology of a 0.60 µm coating exhibits a compact and uniform surface, indicating a complete curing process at 80 °C , Fig. 2 (e) and (f) are the

micro zone morphologies of a coating with a thickness of 0.62 μm formed under a curing temperature of 100 $^{\circ}\text{C}$. As shown in these figures, under a curing condition of PMT=100 $^{\circ}\text{C}$, the coating surface was dense and uniform, and the morphology of galvanized layer pits and the edges of the protruding parts show that the coating covered the Zn layer surface completely, indicating that a coating with a thickness of 0.62 μm can be completely cured at 100 $^{\circ}\text{C}$ [8,9].

For further analyses on the surface morphologies and elements of coatings after curing, a field-emission scanning electron microscope (equipped with an energy dispersive spectrometer) and a X-ray photoelectron spectrometer (XPS) were used, and their results are shown in Fig. 3 and 4. EDS energy spectra and XPS spectra show that the main elements of coating are C, O, Si, Ti, P, and Zn. From the relatively high contents of Si and Zn, combined with the results shown in Figure 1, it can be inferred that the coating and galvanized layer indeed formed better adhesion [7].

Fig. 4 shows the XPS analysis of the coating after passivating and curing. It was found that groups of Si-C, Si-O-Si, Si-O, Si-O-C, Zn-O, C-O, C=O and OH were present in the coating, which is consistent with IR spectra results. In addition, combined with Figure 2 and Figure 3, it can be shown that the coating has a tight three-dimensional network structure on the surface of the galvanized layer that did not spread across the plane.

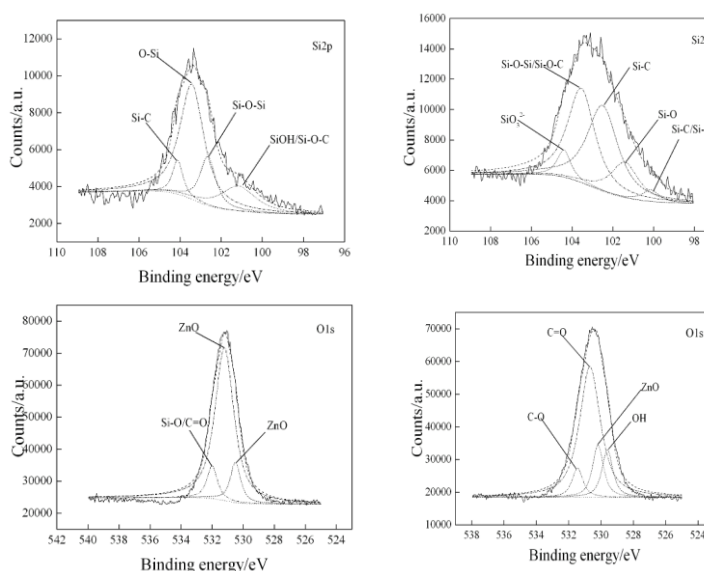


Figure 4. XPS analysis of the coating

3.3 Effect of curing temperature on corrosion resistance

Fig. 5 shows the comparison of polarization curves and pitting potentials of coatings with different thicknesses (0.62 μm , 0.60 μm , 0.58 μm , 0 μm) in 3.5% NaCl solution at different curing temperatures (Table 1). Fig. 5 (a) shows the relationship between polarization curve and coating thickness (curing temperature), while fig. 5 (b) shows the pitting potentials (E_p -t) at different corroding times (24 h, 48 h, 72 h and 96 h) [10, 11]. The corrosion potential increased with film

thickness. Pitting potential (EP) and coating thickness were also related; EP reached a higher value when the thickness was 0.60 μm .

The polarization curve parameters for different coating thicknesses are shown in table 2. According to fig. 5 and tab. 2, the corrosion potential increased gradually with film thickness, the E_{corr} of the bare sheet was -457.3 mV, the E_{corr} of the 0.58 μm specimen was 184.1 mV, the E_{corr} of the 0.60 μm specimen was 293.9 mV, and the E_{corr} of the 0.62 μm specimen was 410.5 mV. The corrosion potential of the bare sheet was lowest, and its current stayed larger, while the specimen with 0.62 μm coating thickness had the highest corrosion potential, and its polarization resistance (R_p) reached $2.13 \times 10^6 \text{ ohms}\cdot\text{cm}^{-2}$. To sum up, thicker coatings and better corrosion resistance can be acquired at higher curing temperature.

The results of a neutral salt spray test for a chromium-free composite passivation plate film thickness galvanized sheet sample and a German-brand environmental protection passivation plate HG621 according to GB/T 10125-2012 are shown in Figures 6 (a) and (b). Figure 6 (a) shows the HG621 chromium-free passivation plate, and (b) shows the composite passivation plate sample with a film thickness of 0.62 μm . After a 96-h salt spray test (NSS), the percent surface area of the composite coating sample was <1%, while the percent corrosion area of the HG621 passivation hot-dip galvanizing plate was 3%. The surface of a hot dip galvanized sheet coated with tannic acid- H_2TiF_6 /silica sol has excellent corrosion resistance, and its corrosion resistance can be equivalent to the other commercial environmental protection passivation hot galvanized sheet.

Compared with the results of other studies[8,9,13], a passive film composed of low cost raw materials (Tannins, Fluotitanic acid and Nanosilica Sol) can form a passivating film with the same corrosion resistance as found in this study. The thickness of the thickest film is only 0.62 μm , and a curing temperature between 80 $^\circ\text{C}$ to 100 $^\circ\text{C}$ can reach comparable corrosion resistance to the HG621 chromium-free passivating film of a well-known international brand (Henkel). Comparative analyses of electrochemical polarization curves and salt spray tests were conducted, and the results strongly prove that the developed passivating films have more practical application value. This finding provides favorable evidence and experimental support for subsequent industrial development and application.

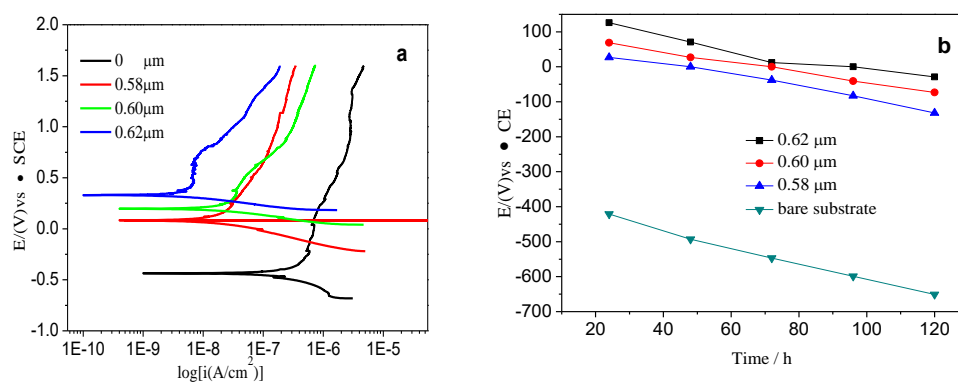
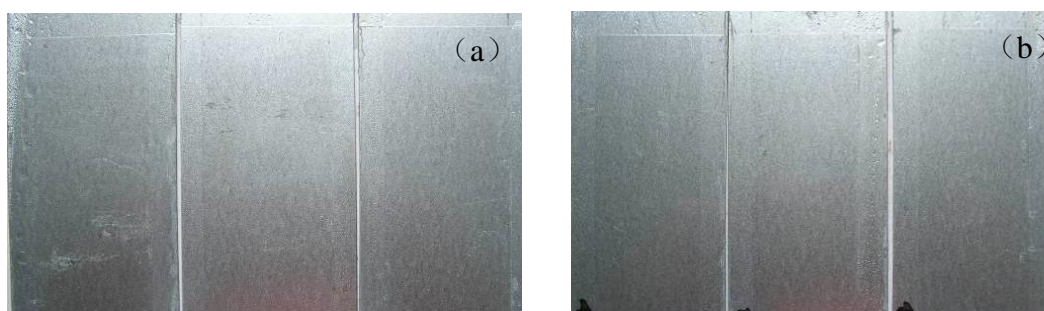


Figure 5. Comparison of the polarization curves and pitting potentials of coatings with different thicknesses on hot-dip galvanized steel sheets, tested in 3.5 g/l NaCl solution

Table 2. Parameters of the polarization curves for different coating thicknesses

Film thickness (μm)	$E(\text{corr})$ (mV)	$I(\text{corr})$ ($\text{A}\cdot\text{cm}^{-2}$)	R_p ($\text{ohms}\cdot\text{cm}^{-2}$)
0	-457.3	0.61×10^{-6}	0.79×10^5
0.58	184.1	3.88×10^{-7}	3.80×10^5
0.60	293.9	0.71×10^{-7}	8.14×10^5
0.62	410.5	9.30×10^{-8}	2.13×10^6

**Figure 6.** Corrosion test results after 96 hrs of NSST a. Coating thickness of $1.0\ \mu\text{m}$ with HG621; b. Coating thickness of $0.62\ \mu\text{m}$

4. CONCLUSIONS

1) Tannic acid-fluoro titanate acid-silane environmental protection passivating solution can chemically bond with the substrate surface of a galvanized steel layer, producing an Si-O-Zn bond instead of a simple physical deposition. An Si-O-Si bond can form through condensation between silanol Si-OH, thereby making it possible to form coatings on the surfaces of hot dip galvanized steel sheets by passivating materials and processes;

2) After passivation and curing treatments, the coatings became more dense, and their surfaces became smooth, uniform, and flat, with no edges and corners. The main elements found in the coatings were O, Si, S, C and Zn;

3) Corrosion potential increased gradually with curing temperature and coating thickness, with a coating thickness of $0.62\ \mu\text{m}$ at 100°C . At this thickness, the corrosion potential E_{corr} reached its highest value at 410.5 mV, impedance R_p was measured to be $2.13 \times 10^6\ \text{ohms}\cdot\text{cm}^{-2}$, and the coating provided great corrosion resistance.

ACKNOWLEDGEMENTS

One of the authors (Mr. Xu Zhefeng) gratefully acknowledges financial support from Ministry of Science and Technology of the People's Republic of China, through 863 Project (No. 2009AA03Z529). The authors wish to acknowledge Prof. Yan Chuanwei, Institute of Metal Research, Chinese Academy of Sciences, for providing the electrochemical measurement system facility.

References

1. S.M.A. Shibli, B.N.Meena, R.Remya, *Surf. Coat. Technol.*, 262 (2015) 210.
2. H. Yang, S. Zhang, J. Li, X. Liu, H. Wang, *Surf. Coat. Technol.*, 240 (2014) 269.
3. Z. F. Xu, S. Liu, G. Y. Gan, J. H. Yi, *Optoelectron. Adv., Mater. –Rapid Comm.*, 9 (2015)1487-1490.
4. Z. Chen, C.T. Peng, Q. Liu, R. Smith, D. Nolan, *J. Alloys Compd.*, 589 (2014) 226.
5. Y. Gui, Q. Xu, Y. Guo, *J. Iron Steel Res. Int.*, 21 (3) (2014) 396.
6. J. Duchoslav, M. Arndt, R. Steinberger, T. Keppert, G. Luckeneder, K.H. Stellnberger, J. Hagler, C.K. Riener, G. Angeli, D. Stifter, *Corros. Sci.*, 83 (2014) 327.
7. Hsiang-Yu Su, Pei-Li Chen, Chao-Sung Lin, *Corros. Sci.*, 102(2016) 63.
8. M. Poelmana, M. Fedel,C.Motte,D.Lahem, Th. Urios,Y.Paint,F.Deflorian, M.-G. Olivier, *Coat. Technol.*, 274 (2015) 1.
9. M. Poelmana, M. Fedel,C.Motte,D.Lahem, Th. Urios,Y.Paint,F.Deflorian, M.-G. Olivier, *Coat. Technol.*, 274 (2015) 9.
10. Yuanwei Liu, Yu Chen, *Int. J. Electrochem. Sci.*, 13 (2018) 530.
11. S.M. Mousavifard, M.M. Attar, A. Ghanbari, M. Dadgar, *J. Alloys Compd.*, 639 (2015) 315.
12. D. Persson, D. Thierry, O. Karlsson, *Corros. Sci.*, 126(2017) 152.
13. Zhiqiang Gao, Dawei Zhang, Xiaogang Li, Sheming Jiang, Qifu Zhang, *Colloids Surf., A* 546 (2018) 221.

© 2018 The Authors. Published by ESG (www.electrochemsci.org). This article is an open access article distributed under the terms and conditions of the Creative Commons Attribution license (<http://creativecommons.org/licenses/by/4.0/>).